Home   Search   Collections   Journals   About   Contact us   My IOPscience

Can near-edge structure of the Bi L$_3$ edge determine the formal valence states of Bi?

Can near-edge structure of the Bi L$_3$ edge determine the formal valence states of Bi?

Nan Jiang and John C H Spence

Department of Physics and Astronomy, Arizona State University, Tempe, AZ 85287-1504, USA

Abstract
We analyse the manner in which local atomic structure affects the identification of Bi valence states in the x-ray absorption near-edge structure (XANES) of the Bi L$_3$ edge, by comparing simulations of the Bi L$_3$ edges in various polymorphs of Bi_2O_3, $NaBiO_3$ and $Ag_{25}Bi_3O_{18}$. We find that while the XANES is certainly sensitive to the ionicity of Bi, it is better described in terms of its sensitivity to the local bond lengths and coordination associated with the valence states of Bi.

1. Introduction

The valence state of Bi in bismuth-containing crystals and glasses has attracted scientific interest for many years, due to its important role in metal-to-insulator transition [1], superconductivity [2] and photoluminescence [3]. In experiments, x-ray absorption near-edge structure (XANES) of the Bi L$_3$ edge has been extensively used to determine the valence state of Bi in various crystals and glasses [4–21]. These measurements usually require a comparison with standard samples (e.g. Bi_2O_3 and $NaBiO_3$) of known oxidation states. This assumes that the differences between Bi L$_3$ XANES are due to differences in Bi valence state, without theoretical justification.

It is known that the XANES, as well as electron energy-loss near-edge structure (ELNES), is sensitive to both local structure and chemistry. It has been general practice to use XANES and ELNES to study valence states, such as those in transition metal oxides [22, 23]. In some cases, however, XANES and ELNES are clearly more sensitive to local structure than to the valence state. For example, B has the formal valence B^{3+} in oxides, regardless of its threefold or fourfold coordination to O. However, the XANES and ELNES of the B K edge are significantly different in these two coordination forms, and this has been widely used as a fingerprint to distinguish the local structural environment around the B [24, 25]. In the heavy element oxide TeO_2, the local structure gradually evolves from a [TeO_4] trigonal bipyramid to a [TeO_3] trigonal pyramid when other metal oxides (e.g. Nb_2O_5) are added, although the formal valence of Te remains Te^{4+}. This structural change can be identified via the disappearance of a small peak within 10 eV of the threshold of the Te L$_3$ edge [26]. Therefore, it is necessary

Table 1. A list of Bi–O distances in the first shell in various compounds. The data in the parentheses are excluded from calculating the average bonding distances. o-Bi_2O_3 represents the orthorhombic phase.

		Bi–O distances (Å) in the first shell	Average
α-Bi_2O_3 [33]	(Bi1)	2.075, 2.174, 2.209, 2.548, 2.636, (3.244)	2.329
	(Bi2)	2.136, 2.224, 2.290, 2.477, 2.531, (2.796)	2.332
β-Bi_2O_3 [34]		2.096, 2.128, 2.253, 2.463, (2.720), (2.978)	2.235
γ-Bi_2O_3 [31]	(Bi1)	2.087, 2.234, 2.283, 2.595, 2.622, (3.117)	2.364
	(Bi2)	1.910, 1.910, 1.910, 1.910	1.910
δ-Bi_2O_3 [31]		2.451, 2.451, 2.451, 2.451	2.451
o-Bi_2O_3 [32]		2.082, 2.170, 2.173, 2.489, 2.569, (3.473)	2.297
$NaBiO_3$ [35]		2.094, 2.094, 2.094, 2.137, 2.137, 2.137	2.116
$Ag_{25}Bi_3O_{18}$ [36]	(Bi1)	2.207, 2.207, 2.207, 2.507, 2.507, 2.507	2.357
	(Bi2)	2.130, 2.130, 2.130, 2.130, 2.130, 2.130	2.130

to justify theoretically whether the XANES of the Bi L_3 edge is more sensitive to its formal valence state or to the structural environment around Bi.

In this work, we discuss how local structures affect the identification of Bi valence states in the XANES of the Bi L_3 edge, by comparing simulations of the Bi L_3 edges in various polymorphs of Bi_2O_3, $NaBiO_3$ and $Ag_{25}Bi_3O_{18}$.

2. Theoretical calculations

The XANES simulations were carried out using a real-space multiple scattering (MS) approach, as encoded in the FEFF8 algorithm [27]. The wavefunctions were obtained by solving the Dirac equation self-consistently in the relativistic spinor representation using muffin-tin potentials. For the DOS calculations, the ground state von Barth–Hedin exchange–correlation potential [28] was used. The Hedin–Lundqvist energy-dependent self-energy correction [29] was added to the SCF total energy in the simulations of the XANES. The core hole effect is also included using the 'frozen core hole' approximation. The radius of the cluster for multiple scattering during the self-consistency loop is 7 Å, which contains about 100 atoms. The maximum values of the angular momentum basis are $l_{max} = 1$ for oxygen and 3 for bismuth. The maximum value of the overlap for the muffin tins is 10%.

Bi_2O_3 has several polymorphs, including the α-, β-, γ-, δ-, and o-Bi_2O_3 phases [30–32]. Accordingly, Bi in these polymorphs should bear the formal valence charge of Bi^{3+}.

α-Bi_2O_3: This is the most stable form at room temperature. Bismuth has two inequivalent positions in α-Bi_2O_3: both are considered to be fivefold coordinated to O. The coordination surrounding Bi may be described as a distorted octahedron, with one of its corners removed. The Bi–O bond distances are listed in table 1 [33].

β-Bi_2O_3: Although six O surround Bi in this structure, two of them are almost 3 Å away from Bi (table 1) [34]. Therefore, the O polyhedron surrounding Bi may be described as a pseudo-trigonal bipyramid.

γ-Bi_2O_3: This is isomorphous with the bcc $Bi_{12}GeO_{20}$ [31]. The Bi atoms in pure γ-Bi_2O_3 occupy positions which are tetrahedrally coordinated to O, and normally occupied by the impurity (e.g. Ge) ion. Therefore, there are two inequivalent Bi atoms in γ-Bi_2O_3: one is fivefold coordinated to O, resembling that in α-Bi_2O_3; another is fourfold coordinated to O. The Bi–O bond distances are listed in table 1.
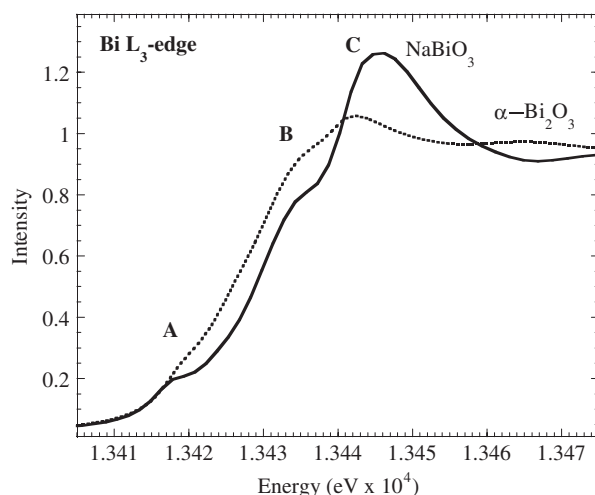
Figure 1. Comparison of calculations for Bi L$_3$ edges in α-Bi$_2$O$_3$ and NaBiO$_3$.

δ-*Bi$_2$O$_3$*: This cubic δ form is the high-temperature phase. There is some controversy concerning the structure and space group [30, 31]. As regards the local structure of Bi, however, there is general agreement that Bi is fourfold coordinated to O with a relatively long Bi–O distance (table 1). In this work, we used the lattice and atom position parameters given by Medernach [30].

o-Bi$_2$O$_3$: This is an orthorhombic phase. The local environment surrounding Bi can be derived from the fluorite structure, in which three O atoms at the corner of the cube are removed and the remaining five O atoms are displaced [32].

The calculations were also carried out for two other structures: NaBiO$_3$ (Bi^{5+}) and Ag$_{25}$Bi$_3$O$_{18}$ (Bi^{3+} and Bi^{5+}). The crystal structure of NaBiO$_3$ consists of BiO$_6$ octahedra and NaO$_6$ octahedra, and the mean Bi–O distance is about 2.12 Å [35]. Ag$_{25}$Bi$_3$O$_{18}$ contains both Bi^{3+} and Bi^{5+} [36]. Bi^{3+} is in a distorted O octahedron, with three O at a distance of 2.21 Å and the other three at a distance of 2.51 Å. Bi^{5+} lies almost within a regular O octahedron, at an equal distance of 2.13 Å, which is in agreement with the other Bi^{5+} bismuth oxides, such as NaBiO$_3$.

3. Results and discussion

Overall, the XANES of the Bi L$_3$ edge consists of a main peak with delayed maximum intensity [4–21]. There are three major features in this broad peak (indicated A, B and C). All these features have been used to identify the formal valence states of Bi [4–21]. For NaBiO$_3$, the small peak A is significantly stronger in comparison with that for α-Bi$_2$O$_3$, where it is only a slight bump. Therefore, it is always considered to be characteristic of Bi^{5+} [4–21]. There is also a shift of about 2 eV to higher energy in the general position of the absorption edge for NaBiO$_3$, compared to α-Bi$_2$O$_3$. As a result, the energies of peaks B and C for NaBiO$_3$ are higher than those for α-Bi$_2$O$_3$. Figure 1 compares simulations of the Bi L$_3$ edge in α-Bi$_2$O$_3$ and NaBiO$_3$, which are often used as standards for Bi^{3+} and Bi^{5+}, respectively. The calculated Bi L$_3$ edge in α-Bi$_2$O$_3$ is the average of two inequivalent sites. In our calculations, all these characteristics are qualitatively reproduced, although differences exist. For NaBiO$_3$, the major discrepancy is as regards the position of peak C. For Bi$_2$O$_3$, the calculated intensity of peak A is slightly stronger than those from experiments. Both effects are probably due to the use of muffin-tin potentials
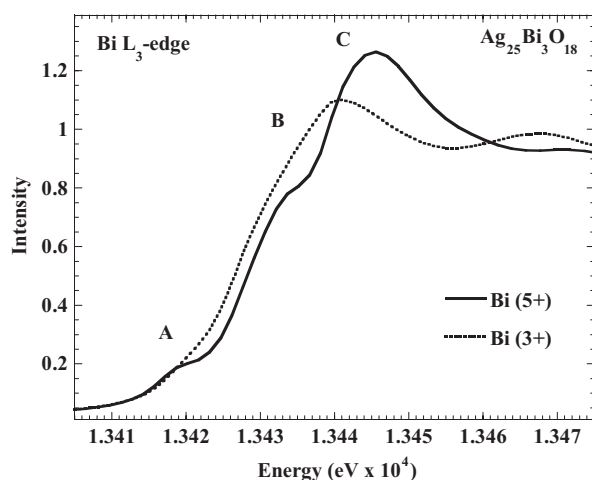
Figure 2. Comparison of the calculated Bi L_3 edge for Bi^{3+} and Bi^{5+} in $Ag_{25}Bi_3O_{18}$.

in the calculations [37]. Later, it will be shows that slight variations in Bi–O bond lengths may also cause these discrepancies. Nevertheless, for the purposes of distinguishing the formal valence states between Bi^{3+} and Bi^{5+}, our agreement between calculation and experiment is generally satisfactory.

Differences between Bi^{3+} and Bi^{5+} have also been confirmed by calculations for a single compound $Ag_{35}Bi_3O_{18}$, in which Bi has both 3+ and 5+ formal valence states [36]. The results are compared in figure 2. This shows that peak A is much stronger for Bi^{5+} than for Bi^{3+}, and the general position of the absorption edge shifts to a higher energy for the former. These results are consistent with the results for Bi_2O_3 and $NaBiO_3$ in figure 1. Interestingly, the two types of Bi have similar coordination, but different mean Bi–O distances (table 1). The mean Bi–O distance of Bi^{5+} in $Ag_{25}Bi_3O_{18}$ is 2.13 Å, which is about the same value as for the other Bi^{5+} oxides: 2.12 Å in $NaBiO_3$ and $AgBiO_3$, 2.10 Å in $KBiO_3$, 2.11 Å in $LiBiO_3$, and 2.10 Å in $MgBi_2O_6$. In contrast, the mean Bi–O distance of Bi^{3+} is about 2.36 Å, which is about the same as that in α-Bi_2O_3 (2.33 Å). Since no charge states were imposed on the Bi in the calculations, we believe that the differences in the calculated spectra in figure 2 are the result of different Bi–O distances.

Peak A was always assigned to the $2p^{3/2} \rightarrow 6s$ transition, since Bi 6s is considered to be empty in Bi^{5+}. By contrast, Bi 6s is filled in Bi^{3+}, and thus this bump is absent. The assignment of the Bi L_3 edge in these compounds is examined in our calculations in figure 3, in which the s and d DOS (density of states) projected on Bi in both $NaBiO_3$ and α-Bi_2O_3 are compared. It is seen that a sharp peak (indicated by arrows in figure 3) occurs near the band gap in the empty s states for $NaBiO_3$, while it is weak and broad for α-Bi_2O_3. However, the Bi 6s state is not completely filled in α-Bi_2O_3. There are comparable intensities of the Bi 6s and 6d empty state DOS near the band gap region, which are both responsible for a small bump in the calculated spectrum for α-Bi_2O_3. The other features of the Bi L_3 edge (peak B and C) are exclusively due to the Bi $2p^{3/2} \rightarrow 6d$ transition. For $NaBiO_3$, the gap between the occupied and empty d DOS is quite large ($\sim$6–8 eV), and the empty 6s is in the middle of the gap. By contrast, the corresponding gap is very small in α-Bi_2O_3. As a result, the edge and the maximum of the main peak (due to transitions to Bi d states) are about 2 eV lower for $NaBiO_3$ than for α-Bi_2O_3. In summary, the XANES of the Bi L_3 edge is largely determined by the empty Bi d DOS, while the empty Bi s DOS only makes contributions in the onset region.
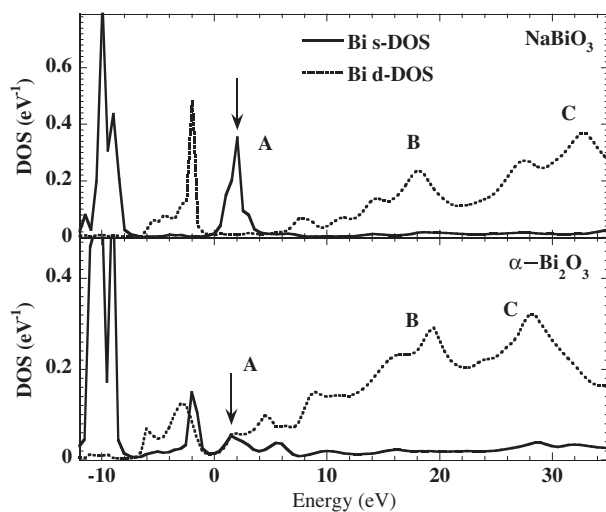
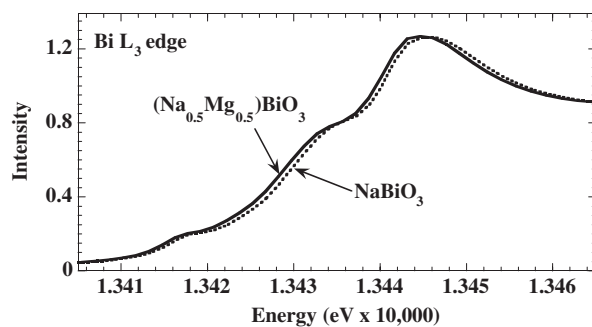**Figure 3.** Comparison of the electronic partial DOS of Bi s and d orbitals in α-Bi$_2$O$_3$ and NaBiO$_3$.

Figure 4. Comparison of the calculated Bi L$_3$ edge in artificial (Na$_{0.5}$Mg$_{0.5}$)BiO$_3$ (solid line) with that in NaBiO$_3$ (dotted line).

In practice, it is always assumed that the gradual change of peak A at the onset region is induced by the change in the formal valence state of Bi [4–21]. Doping electrons in NaBiO$_3$ would fill the empty Bi 6s states, and thus reduce the intensity of peak A. On the other hand, doping holes in α-Bi$_2$O$_3$ would increase the intensity of peak A. Some researchers have also attempted to quantify the Bi valence from the intensity variation of peak A, under the assumption that there is no interaction between the Bi 6s and 6d orbits [20]. To justify this practice, we also carried out calculations for an artificial cluster of NaBiO$_3$, in which half of the Na atoms are randomly replaced by Mg (i.e. Na$_{0.5}$Mg$_{0.5}$BiO$_3$) without change of structure parameters. The result is compared with the calculation for NaBiO$_3$ in figure 4. It shows little difference between these two calculated spectra. The slight shift in energy is probably due to the shift of Fermi energy.

As we know, doping may also cause changes of lattice parameters. To show the relationship between the XANES of the Bi L$_3$ edge and the Bi–O bond distances, we have carried out calculations on modified structural models of α-Bi$_2$O$_3$ and NaBiO$_3$, in which the lattice parameters are slightly decreased and increased, respectively. The results are shown in
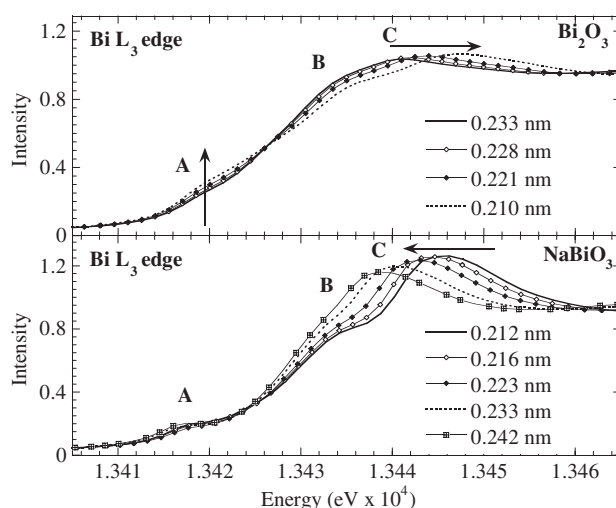
Figure 5. Variation of the Bi L_3 edge with bond distances in α-Bi$_2$O$_3$ and NaBiO$_3$. The arrows indicate the trend of decreasing (upper panel) and increasing (lower panel) bond length.

figure 5. It is seen that a slightly decreasing Bi–O bond distance in α-Bi$_2$O$_3$ results in both peaks B and C shifting toward higher energy, while a slightly increasing Bi–O bond distance in NaBiO$_3$ shifts peak C toward lower energy. This is generally consistent with Natoli's rule that the peak locations in energy are inversely correlated with the bond length [38].

Finally, figure 6 also compares our calculations for the various polymorphs of Bi$_2$O$_3$. In these polymorphs, all the Bi should have the same formal valence charge, Bi^{3+}, except Bi1 in γ-Bi$_2$O$_3$. However, the differences between the XANES among the Bi^{3+} polymorphs are obvious, including the different intensities of the small bump A, as well as the general positions of the absorption edge and the position of peak C. In α-Bi$_2$O$_3$, for example, the two Bi sites (Bi1 and Bi2) have slightly different local structural environments. As shown in table 1, the average O–Bi1 bond distance is slightly smaller than that of O–Bi2. As shown in figure 6, the difference in calculated L_3 edge between Bi1 and Bi2 is not negligible, although all the Bi in α-Bi$_2$O$_3$ is considered to be Bi^{3+}. The small bump in Bi1 is more visible in the region of peak A by comparison with that of Bi2. This small bump cannot be misinterpreted as the peak A of Bi^{5+}, but it can definitely induce errors if quantifying valence is attempted. Additionally, the position of peak C of Bi1 shifts slightly toward higher energy relative to that of Bi2. Therefore, one should be cautious when using the shifts of peaks B and C to identify the valence states of Bi.

On closer inspection, we see that the higher the energy of peak C, the more intense the small bump A becomes. As regards the position of peak C, it apparently increases in the sequence δ-Bi$_2$O$_3$, γ-Bi$_2$O$_3$ (Bi1), α-Bi$_2$O$_3$ (Bi2), α-Bi$_2$O$_3$ (Bi1), β-Bi$_2$O$_3$ and o-Bi$_2$O$_3$. By contrast, the mean Bi–O distance decreases in the same manner in these polymorphs (table 1). This suggests that the XANES of the Bi L_3 edge depends on the near-neighbour distances, as well as on the coordination. Small variation of the local structure can alter the valence state significantly. Therefore, the concept of formal valence charge of Bi is an oversimplified view of the density of states for valence electrons [6].

The mean Bi–O distance for Bi2 is much shorter than that of Bi1 in γ-Bi$_2$O$_3$ (table 1). It has been suggested that Bi2 is most likely to be Bi^{5+} in this polymorph [39]. However, previous attempts to verify its existence were unsuccessful [30]. In our calculations (figure 6), the differences between the Bi L_3 edges around these two different Bi are very similar to the
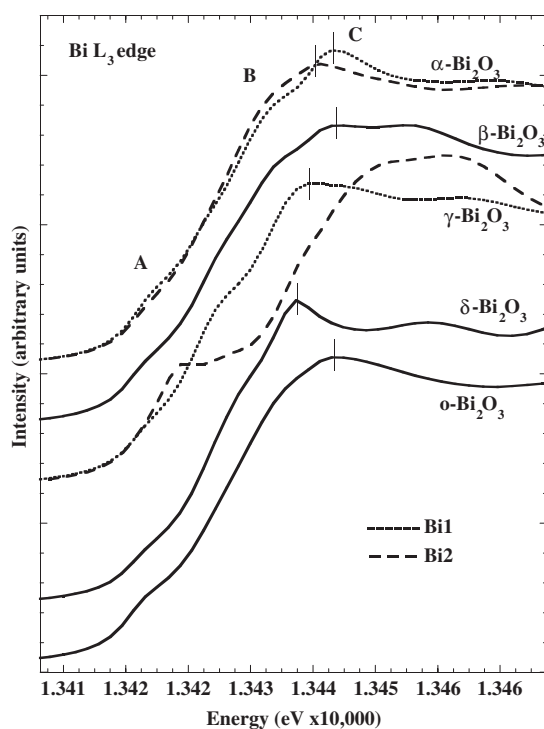
Figure 6. Comparison of calculated Bi L$_3$ edges in various Bi$_2$O$_3$ polymorphs. For α- and γ-Bi$_2$O$_3$, the dotted and chain lines represent the inequivalent sites Bi1 and Bi2, respectively. The vertical lines indicate the positions of peak C.

differences found in calculations for α-Bi$_2$O$_3$ (Bi^{3+}) and NaBiO$_3$ (Bi^{5+}) shown in figure 1, and between Bi^{3+} and Bi^{5+} in Ag$_{25}$Bi$_3$O$_{18}$. These include a significant peak A and lower energies for peaks B and C in Bi2 relative to Bi1. This result provides evidence that Bi2 is most likely to be Bi^{5+}. This conclusion in fact reflects nothing but the fact that the Bi2–O bond distance is much shorter than that of Bi1–O.

We also noted that the Bi L$_3$ edge XANES is very broad, probably due to the short core hole lifetime. The natural width of the Bi L$_3$ level is about 6 eV [40]. Unlike for the relatively light elements, such as for V and Ti L$_{23}$ edges in different V and Ti oxides [22, 23], the differences in the Bi L$_3$ XANES are thus not drastic in the formal valence forms of Bi^{3+} and Bi^{5+}. The change of Bi L$_3$ XANES induced by the change of the local structure alone cannot be distinguished from the change induced by the different formal valence state (figure 5).

4. Conclusion

These simulations confirm that the XANES of the Bi L$_3$ edge is sensitive to the ionicity of Bi (Bi^{3+} or Bi^{5+}), and can indeed be used to distinguish these two states. It is also found that the formal valence of Bi is correlated with its local structure: the Bi^{5+}–O bond distance is shorter than the Bi^{3+}–O bond distance. Therefore the XANES shape can equally better be interpreted as resulting from the change in bond distance and coordination associated with these two atomic configurations. However, even though the formal valence of Bi remains unchanged, small variations in bond distance and coordination can significantly alter the density of states of

valence electrons, and thus the XANES of the Bi L_3 edge. It is therefore preferable to describe the spectra in terms of the local structure around Bi, rather than the formal valence charge of Bi.

Acknowledgment

References

[1] Cox D E and Sleight A W 1979 *Acta Crystallogr.* B **35** 1
[2] Sato H, Tajima S, Takagi H and Uchide S 1989 *Nature* **338** 241
[3] Meng X, Qiu J, Peng M, Chen D, Zhao Q, Jiang X and Zhu C 2005 *Opt. Express* **13** 1628
    Meng X, Qiu J, Peng M, Chen D, Zhao Q, Jiang X and Zhu C 2005 *Opt. Express* **13** 1635
[4] Heald S M, DiMarzio D, Croft M, Hegde M S, Li S and Greenblatt M 1989 *Phys. Rev.* B **40** 8828
[5] Boyce J B, Bridges F G, Claeson T, Geballe T H and Remeika J M 1990 *Phys. Rev.* B **41** 6306
[6] Salem-Sugui S Jr, Alp E E, Mini S M, Ramanathan M, Campuzano J C, Jennings G, Faiz M, Pei S, Dabrowski B,
    Zheng Y, Richards D R and Hinks D G 1991 *Phys. Rev.* B **43** 5511
[7] Li S, Greenblatt M, Jeon Y, Chen J, Liang G and Croft M 1991 *Physica* C **173** 239
[8] Akhtart Z N, Akhtart M J and Catlow C R A 1993 *J. Phys.: Condens. Matter* **5** 2643
[9] Guyot H, Filippini Cl and Marcus J 1993 *J. Alloys Compounds* **195** 543
[10] Liang G, Sahiner A, Croft M, Xu W, Xiang X D, Badresingh D, Li W, Chen J, Peng J, Zettl A and Lu F 1993
    Phys. Rev. B **47** 1029
[11] Pham A Q, Studer F, Merrien N, Maignan A, Michel C and Raveau B 1993 *Phys. Rev.* B **48** 1249
[12] Faiz M, Jennings G, Campuzan J C, Alp E E, Yao J M, Saldin D K and Yu J 1994 *Phys. Rev.* B **50** 6370
[13] Demourgues A, Dussarrat C, Bontcher R, Darriet B, Weill F and Darriet J 1995 *Nucl. Instrum. Methods Phys.
    Res.* B **97** 82
[14] Studer F, Pelloquin D, Maignan A, Michel C, Hervieu M and Raveau B 1995 *Physica* C **242** 1
[15] Pelloquin D, Michel C, Hervieu M, Studer F and Raveau B 1996 *Physica* C **257** 195
[16] Kim D K, Choy J H, Osada M, Kalihana M and Yoshimura M 1998 *Solid State Ion.* **108** 291
[17] Mizoguchi H, Hosono H, Kawazoe H, Yasukawa M, Fujitsu S and Fukumi K 1999 *Mater. Res. Bull.* **34** 373
[18] Choy J H, Hwang S J and Lee W 1999 *J. Solid State Chem.* **142** 199
[19] Allix M, Pelloquin D, Studer F, Nguyen N, Wahl A, Maignan A and Raveau B 2002 *J. Solid State Chem.* **167** 48
[20] Baranov A N, Kim J S, Kim D C, Suh D S, Park Y W and Antipov E V 2002 *Physica* C **383** 95
[21] Liang G, Yao Q, Zhou S and Katz D 2005 *Physica* C **424** 107
[22] Chen J G 1997 *Surf. Sci. Rep.* **30** 1
[23] Leapman R D, Grunes L A and Fejes P L 1982 *Phys. Rev.* B **26** 614
[24] Garvie L A J, Craven A J and Brydson R 1995 *Am. Mineral.* **80** 1132
[25] Fleet M E and Muthupari S 2000 *Am. Mineral.* **85** 1009
[26] Jiang N and Spence J C H 2004 *Phys. Rev.* B **70** 184113
[27] Ankudinov A L, Ravel B, Rehr J J and Conradson S D 1998 *Phys. Rev.* B **58** 7565
[28] von Barth U and Lundqvist S 1972 *J. Phys. C: Solid State Phys.* **5** 1629
[29] Hedin L and Lundqvist S 1969 *Solid State Phys.* **23** 1
[30] Medernach J W and Snyder R L 1978 *J. Am. Ceram. Soc.* **61** 494
[31] Harwig H A 1978 *Z. Anorg. Allg. Chem.* **444** 151
[32] Kumada N and Kinomura N 1999 *Mater. Res. Soc. Symp. Proc.* **547** 227
[33] Malmros G 1970 *Acta Chem. Scand.* **24** 384
[34] Blower S K and Greaves C 1988 *Acta Crystallogr.* C **44** 587
[35] Kumada N, Kinomura N and Sleight A W 2000 *Mater. Res. Bull.* **35** 2397
[36] Bortz M and Jansen M 1991 *Angew. Chem. Int. Edn Engl.* **30** 883
    Bortz M and Jansen M 1992 *Anorg. Allg. Chem.* **612** 113
[37] Jiang N and Spence J C H 2004 *Phys. Rev.* B **70** 014112
    Jiang N, Jiang B, Erni R, Browning N D and Spence J C H 2006 *Ultramicroscopy* **106** 123
[38] Natoli C R 1983 *EXAFS and Near Edge Structure* ed A Bianconi *et al* (New York: Springer) p 43
[39] Craig D C and Stephenson N C 1975 *J. Solid State Chem.* **15** 1
[40] Krause M O and Oliver J H 1979 *J. Phys. Chem. Ref. Data* **8** 329